CHAPTER 7

REACTIVE CALCINATION: A NOVEL ROUTE FOR IMPROVED ACTIVITY OF THE PEROVSKITE CATALYST

7.1 Introduction

Soot/PM is the major pollutant released from diesel engines used in on-road and off-road applications around the globe. Numerous articles have been reported to control the diesel engine emissions, predominantly soot after-treatment technologies. Catalyst coated DPF is an efficient passive device to trap and burn the diesel soot at low temperature. The performance of the catalysts very much depends upon the conditions for calcination of the precursor and the subsequent activation. Partially reduced catalysts have been reported to be more active than unreduced ones in vehicular pollution control [Severino et al. 1998]. Reduction of the oxide phase of the catalysts is highly exothermic process and therefore great care is required to avoid local overheating. High temperature causes sintering of active crystallites with a consequent loss of surface area and activity. So, the catalyst is reduced under a very controlled condition. To minimize the above mentioned drawbacks of the conventional methods of two step processes of calcination and activation, a newer route of single step reactive-

calcination (RC) of catalyst precursor far below their decomposition temperature is investigated presently for preparing highly active catalysts bypassing the reduction step. Details of RC are described below.

Thus, the objective of the present chapter was to compare the effect of calcination mode in stagnant air and reactive calcination of the precursor. The double-substituted perovskite, $La_{0.9}Sr_{0.1}Co_{0.5}Fe_{0.5}O_{3-\delta}$ were prepared by calcination in stagnant air as well as by RC. The catalysts thus obtained were characterized by various techniques and examined for catalytic performance of the diesel soot combustion.

7.2 Experimental

7.2.1 Preparation of Catalysts

The precursor, of the double substituted perovskite; $La_{0.9}Sr_{0.1}Co_{0.5}Fe_{0.5}O_{3-\delta}$ showing the best activity for soot oxidation was also calcined following the novel route of RC developed in this laboratory, as discussed in the subsequent section. The detailed method of preparation of the precursor has already been discussed in section 6.2.1.

7.2.2 Reactive Calcination of the Catalysts

Reactive calcination of the precursor of double substituted perovskite ($La_{0.9}Sr_{0.1}Co_{0.5}Fe_{0.5}O_{3-\delta}$) was carried out by the introduction of low concentration of chemically reactive CO-air mixture (4.6% CO) at a total flow rate of 60 ml min^{-1} over the hot precursors. The RC was carried out in a down flow bench-scale tubular reactor having a definite amount of the precursor. The reactor was placed in a split open microprocessor temperature controlled furnace. The flow rates of CO and air were monitored using digital gas flow meters to feed the mixture (dried and CO_2 free) in required proportion to the reactor. The temperature of the precursor bed was measured with a thermocouple inserted in the thermo-well of the reactor reaching the bed. The temperature of the bed was increased at a steady rate of heating at 2^oC min^{-1} from room

temperature to 600^{o}C in the flowing environment of CO-air mixture. This temperature was maintained for an hour. Then in the second step of calcination temperature of the bed was increased to 750^{o}C and maintained for another 2h under the same atmosphere. The catalyst was cooled to room temperature in the same atmosphere, collected and stored in an airtight bottle. Nomenclature of the catalysts is given below in table 7.1.

Table 7.1 Nomenclature of the Catalysts

Catalyst (calcination mode)	**Name**
$La_{0.9}Sr_{0.1}Co_{0.5}Fe_{0.5}O_{3-\delta}$ (Air)	Cat-CC*
$La_{0.9}Sr_{0.1}Co_{0.5}Fe_{0.5}O_{3-\delta}$ (RC)	Cat-RC**

** Conventionally calcined; **reactively calcined*

7.2.3 Characterization of the Catalyst Samples

The textural characterization of the catalysts was carried out by low temperature N_2-physisorption method using a Micromeritics ASAP 2020 analyser. Phase identification of the catalysts was done by X-ray diffraction (XRD) patterns recorded on a powder X-ray diffractometer (Rigaku Ultima IV) using CuKα1 (λ = 1.5405 Å) radiation with a nickel filter operating at 40mA and 40kV. The XPS measurement was performed on an Amicus spectrometer equipped with Mg Kα X-ray radiation. For typical analysis, the source was operated at a voltage of 15 kV and current of 12 mA. Pressure in the analysis chamber was less than 10^{-5} Pa. The binding energy scale was calibrated by setting the main C 1s line of adventitious impurities at 284.7 eV, giving an uncertainty in peak positions of ±0.2 eV. FTIR spectra of the catalysts were recorded in the range of 400-4000 cm^{-1} on Shimadzu 8400 FTIR spectrometer with KBr pellets at room temperature. Scanning electron micrographs (SEM) and SEM EDX were recorded on

Zeiss EVO 18 scanning electron microscope (SEM) instrument. An accelerating voltage of 15kV and magnification of 1000X was applied.

7.2.4 Catalytic Performance Measurements

The catalytic performances of the prepared catalysts for oxidation of soot were evaluated in a compact fixed bed tubular quartz reactor shown as in figure 3.9 as described in section 3.6.2. The reactively calcined Cat-RC showing the best activity was examined for its thermal stability by performing the experiment consecutively five times. After complete combustion of soot the catalyst was taken out from the reactor and mixed again with 10 mg of soot under tight contact. The oxidation experiment was repeated as mentioned above, in the same way five cycles of experiments with this catalyst were conducted.

7.3 Results and Discussion

7.3.1 Textural Characterization by N_2-Physisorption

Typical nitrogen physisorption isotherms and pore size distribution curves for the catalyst Cat-CC and Cat-RC are shown in Figures 7.1 and 7.2 respectively. The nitrogen sorption isotherms exhibit type-IV isotherms with H1 type hysteresis loop. This type of isotherm occurs on porous adsorbent with pores in the mesoporous range of 2-25 nm. The desorption curves are practically coincide with adsorption branch of the respective sorption isotherms of all the samples irrespective of the composition of the catalysts. This behaviour is a representative of open textured pores, which offers practically negligible diffusion resistance during the reaction. The pore size distribution curve for Cat-CC presented in figure 7.1 (b) trimodal nature with most probable pores around 40, 140, 220 Å while for cat-RC in figure 7.2 (b) its monomodal with most probable pore around 70 Å.

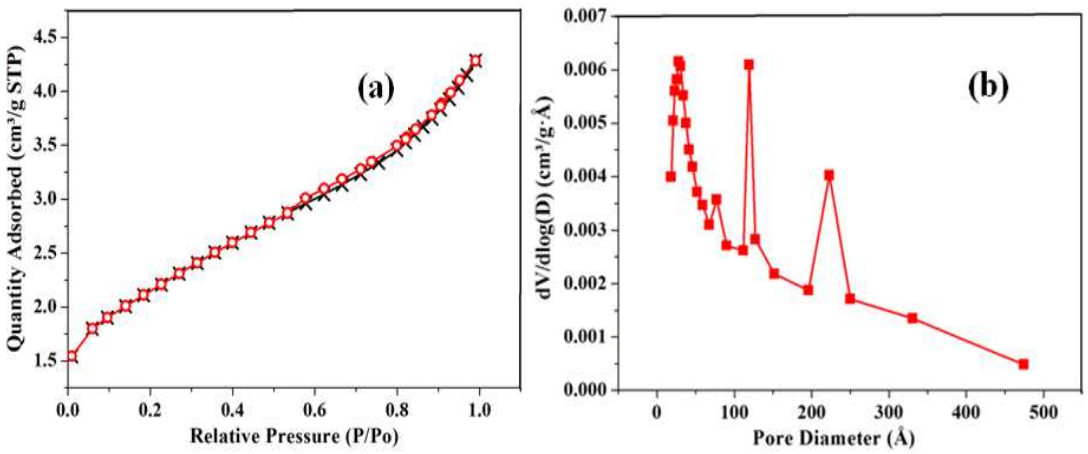

Figure 7.1 (a) N_2 Physisorption isotherms and **(b)** Pore size distribution of Cat-CC

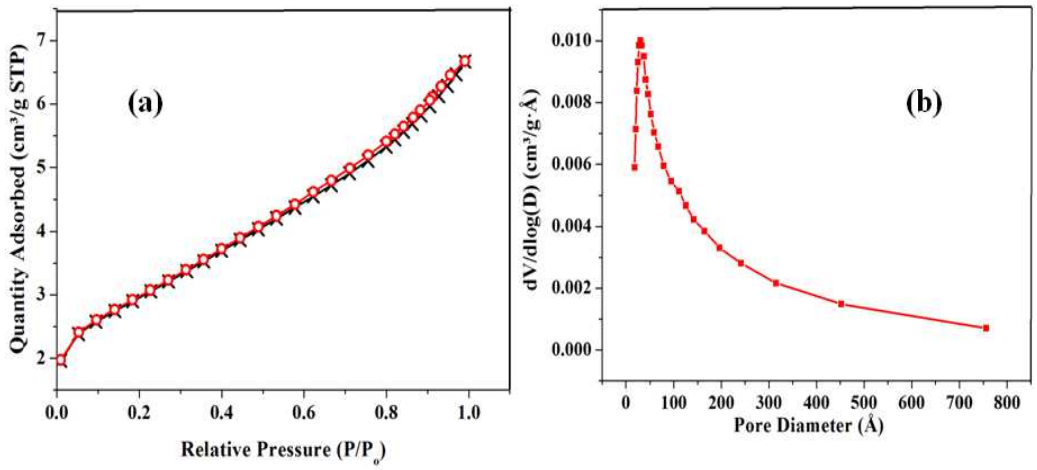

Figure 7.2 (a) N_2 Physisorption isotherms and **(b)** Pore size distribution of Cat-RC

The textural properties including BET surface area, total pore volume and average pore diameter of the perovskite studied in the present investigation are summarized in Table 7.2. It can be seen from the table that the catalyst calcined in air (Cat-CC), displayed the lower surface area than the catalyst calcined reactively (Cat-RC). Cat-CC exhibited the lower pore volume than Cat-RC and comparable average pore diameter.

Table 7.2 Textural Characterization of Perovskite Catalyst samples

Catalyst	Textural Properties			
	S_{BET} (m^2/g)	Pore vol (cm^3/g)	Avg pore size (Å)	Crystallite size (nm)
Cat-CC	7.29	0.0041	6.51	14.09
Cat-RC	7.71	0.0056	6.24	12.42

7.3.2 XRD Analysis of the Catalysts

The powder XRD patterns of catalyst samples are shown in Figure 7.3. The XRD peaks were found to be very sharp indicating that the ABO_3 perovskite structure is well maintained in both the catalysts. The XRD analysis of conventionally calcined in air Cat-CC showed the formation of cubic $LaFeO_3$ structure (JCPDS card No. 00-075-0439) and $LaCoO_3$ (JCPDS card No. 25-1060) with no traces of other phases. For Cat-RC, additional peaks of La_2O_3 (JCPDS card No. 83-1344) were present. The broader peaks in Cat-RC indicate relatively amorphous nature of the catalyst and formation of small crystallites of perovskite. The crystallite size was estimated using the Scherrer equation (3.9) is reported in Table 7.1.

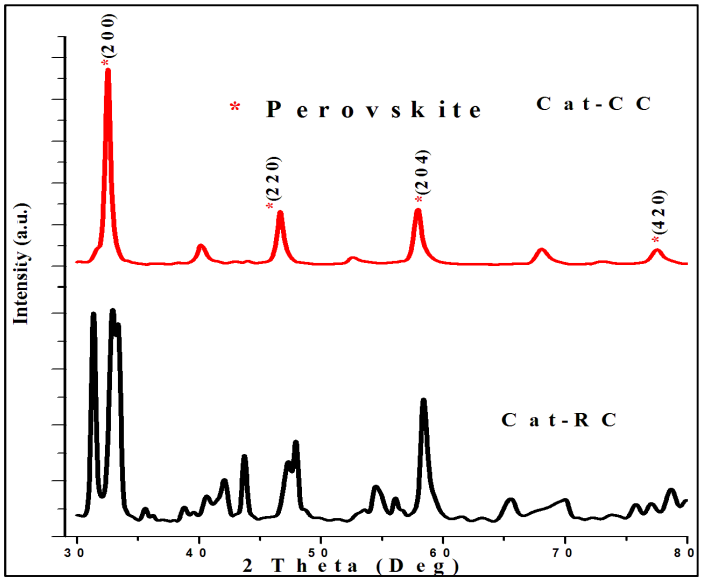

Figure 7.3 X-Ray Patterns of Cat-CC and Cat-RC Perovskite Catalysts

7.3.3 XPS Analysis of the Catalysts

The XPS Spectra of $La_{0.9}Sr_{0.1}Co_{0.5}Fe_{0.5}O_3$ sample calcined in air (Cat-CC) are shown in Figure 7.4. Figure 7.4(a) shows the XPS spectra of La 3d, the peaks of La $3d_{5/2}$ and La $3d_{3/2}$ were situated at 854.2 eV and 857.4 eV and at 837.1 eV and 840.6 eV, respectively. The spin-orbit splitting of La 3d level is 17.0 eV. Figure 7.4 (b) and 7.4 (c) shows the XPS spectra of Co 2p and Fe 2p respectively. The spin-orbit splitting of Co 2p and Fe 2p levels are 15.2 and 12.8 eV which is in well support with the literature. The O 1s energy spectrum consists of two peaks having binding energies 531.2 and 533.8, which correspond to two forms of oxygen, i.e. lattice oxygen and adsorption oxygen respectively as shown in figure 7.4(d).

The characteristic spectra of catalyst Cat-RC are displayed in Figure 7.5, the collected data for La 3d, Co 2p, Fe 2p and O 1s. There exists relatively more adsorption oxygen on the surface indicating the presence of more oxygen vacancies. These adsorption oxygen traps electron and form more active O_2^-. Figure 7.5(a) shows the XPS spectra of La 3d, the peaks of La $3d_{5/2}$ and La $3d_{3/2}$ were situated at 853.3 eV and 856.8 eV and at 836.4 eV and 840.4 eV, respectively. The spin-orbit splitting of La 3d level is 16.4 eV. Fig 7.5(b) and 7.5(c) shows the XPS spectra of Co 2p and Fe 2p respectively. The spin-orbit splitting of Co 2p and Fe 2p levels are 15.2 and 12.8 eV which are in well support with the literature. The O 1s energy spectrum consists of two peaks, which correspond to two forms of oxygen, i.e. lattice oxygen and adsorption oxygen are shown in figure 7.5(d). As in both the catalysts some of La^{3+} was replaced by Sr^+, there were changes in the relative ratio of adsorption to lattice oxygen. More adsorption oxygen existed on the surface indicating the presence of more oxygen vacancies and an increased content of quasi-free electrons in the catalyst. More adsorption oxygen traps more electrons and thus it is favourable for forming more O^{2-}, which becomes more

active centres for oxidation, thus it results in the enhancement in oxidizing ability of the catalyst. It would contribute to the decrease of the combustion temperature of soot particles.

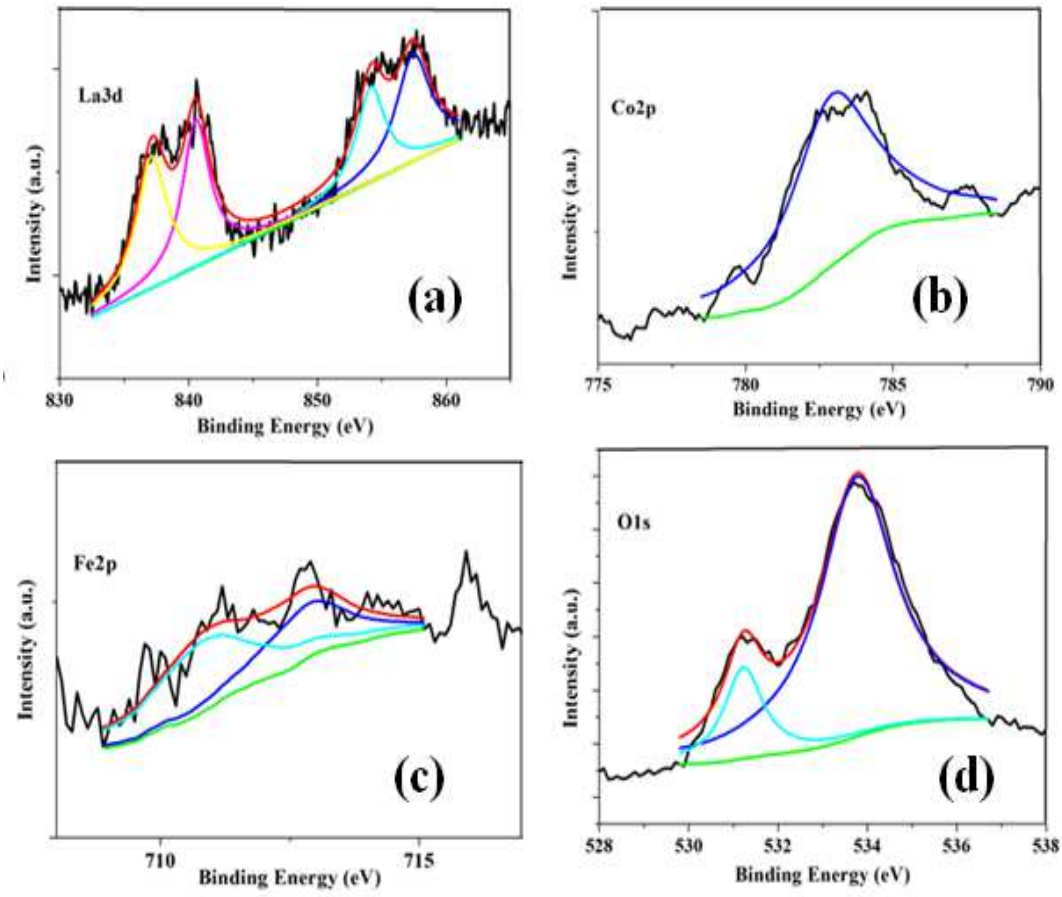

Figure 7.4 XPS Spectra of Cat-CC ($La_{0.9}Sr_{0.1}Co_{0.5}Fe_{0.5}O_{3-\delta}$)

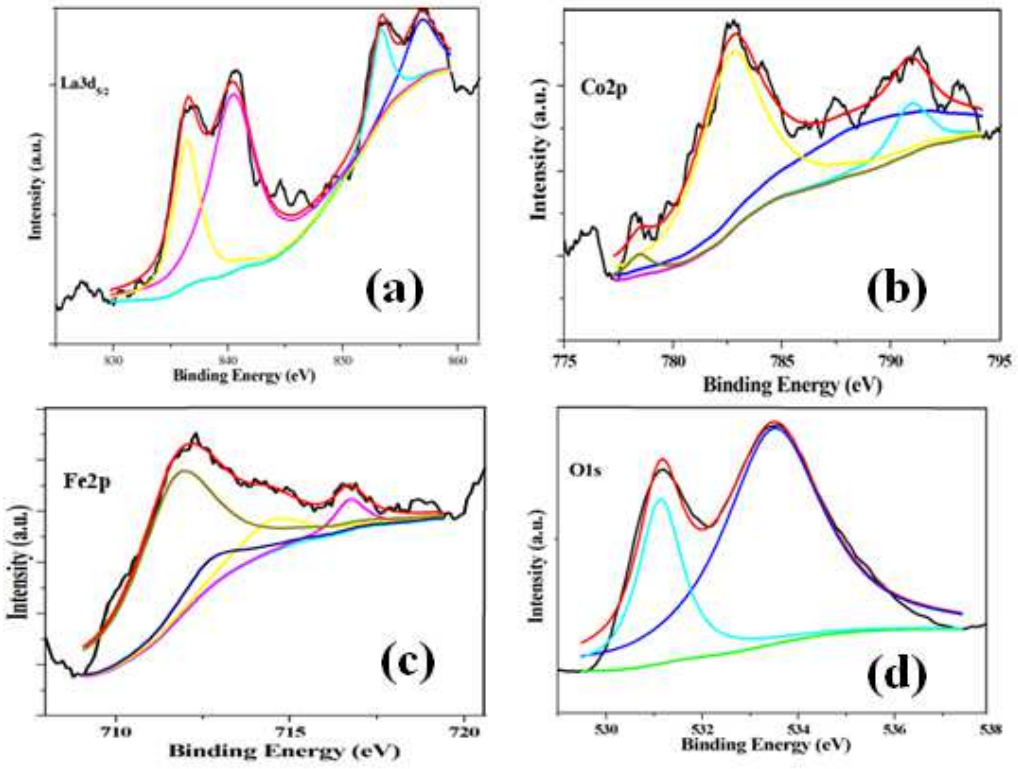

Figure 7.5 XPS Spectra of Cat -RC ($La_{0.9}Sr_{0.1}Co_{0.5}Fe_{0.5}O_{3-\delta}$)

7.3.4 FTIR Characterization of the Catalysts

Figure 7.6 depicts the FTIR spectra of the catalysts calcined at 750^{o}C in stagnant air as well as in reactive mixtures of CO-air. The broader peak appeared in range of 588-594 cm^{-1} is characteristic of the MO_6 octahedra commonly found in perovskite oxide powder and is observed in this system too [Ramesh et al. 1995]. The peaks found near to 2350 cm^{-1} in the samples are due to the presence of atmospheric moisture as reported earlier [Mandelovici et al. 1994]. The absorption band at 1480 and1490 cm^{-1} was corresponded to nitrate ion. In addition, the band at 1100 and 1200 cm^{-1} was corresponded to Co-OH bending which is confirmed with the reported value that MOH bending mode appears below 1200 cm^{-1} [Nakamoto 1997].

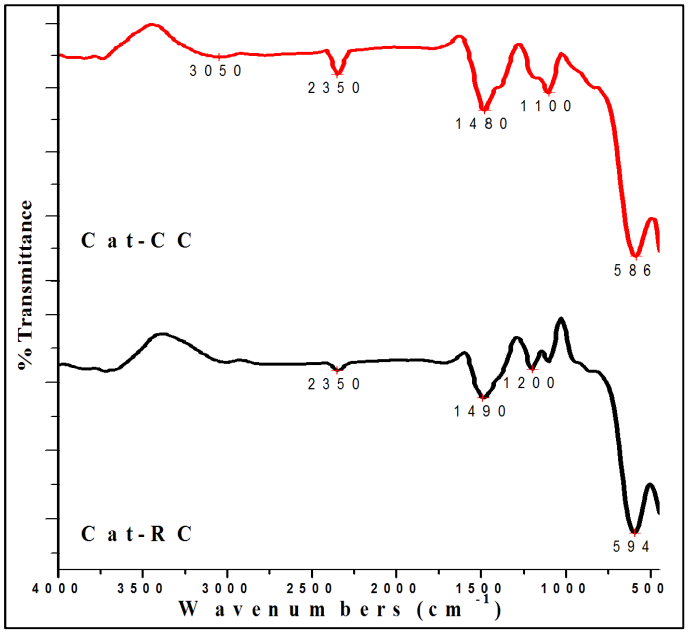

Figure 7.6 FTIR spectra of pure and substituted perovskite catalysts

7.3.5 SEM Characterization of the Catalysts

The SEM micrographs of perovskite catalysts are shown in figure 7.7. It can be seen that the morphologies of particles are of irregular shape and within the nanoscale (<100 nm). The SEM images clearly show the difference in surface morphology by partial substitution of ions. More aggregated porous surface can be visualized in Cat-RC as compare to Cat-CC (figure 7.7A&B). The effects of calcination mode (in air and RC) on the catalyst $La_{0.9}Sr_{0.1}Co_{0.5}Fe_{0.5}O_{3-\delta}$ surface morphology are clearly observed in figure 7.7. Morphological microscopy of the explored samples also demonstrated agglomerates involved mostly thin, smooth flakes and perforated cracked layers having large number of pores.

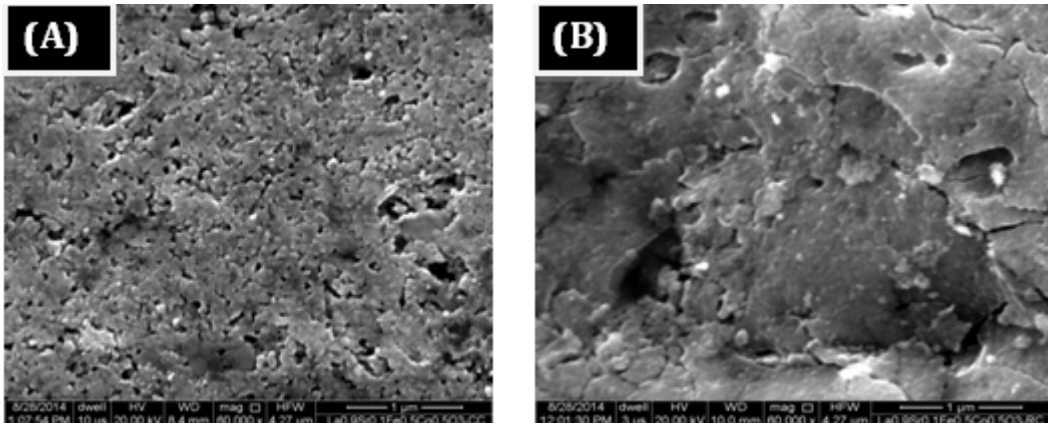

Figure 7.7 SEM images of (A) Cat-CCand (B) Cat-RC perovskite catalyst

7.3.6 Energy Dispersive X-ray (EDX) of the Catalysts

It was evident from the results of energy dispersive X-ray (EDX) analysis that all the samples were pure due to presence of La,Co, Fe and O peak there is no other element present in the spectra as shown in Figure 7.8 It also confirms the presence of Perovskite phase in the sample which is in good harmony with the XRD and XPS experiment results. The theoretical and experimental data (atomic %) of Cat-CC and Cat-RC is shown in table 7.3

Table 7.3 Atomic % data of Cat-CC and Cat-RC

Element	**Cat-CC (Atomic %)**		**Cat-RC (Atomic %)**	
	Theoretical	**Experimental**	**Theoretical**	**Experimental**
O	60	57.54	60	54.53
Fe	10	09.87	10	12.65
Co	10	13.93	10	08.04
Sr	02	1.14	02	02.55
La	18	13.4	18	21.55

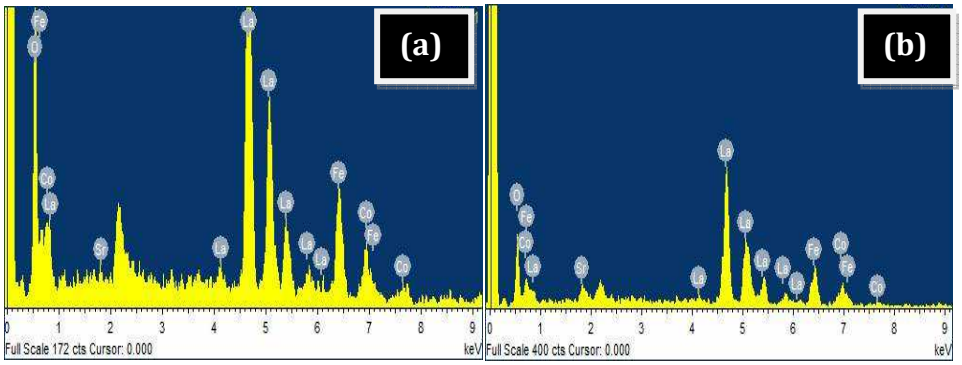

Figure 7.8 EDX spectra of (A) Cat-CC and (B) Cat-RC perovskite catalyst

7.3.7 Catalysts Activity test for Soot Combustion

The activity of the catalyst for soot oxidation was evaluated on the basis of light off temperature characteristics T_i, T_{50} and T_f, i.e. the temperature corresponding to the start of soot ignition, the 50% conversion of soot and complete combustion of soot respectively. Experiments were conducted to examine the effects of partial substitution of La by Sr and of Co by Fe on the activities of the resulting catalysts. The effect of calcinations mode of stagnant air and reactive calcination were also investigated.

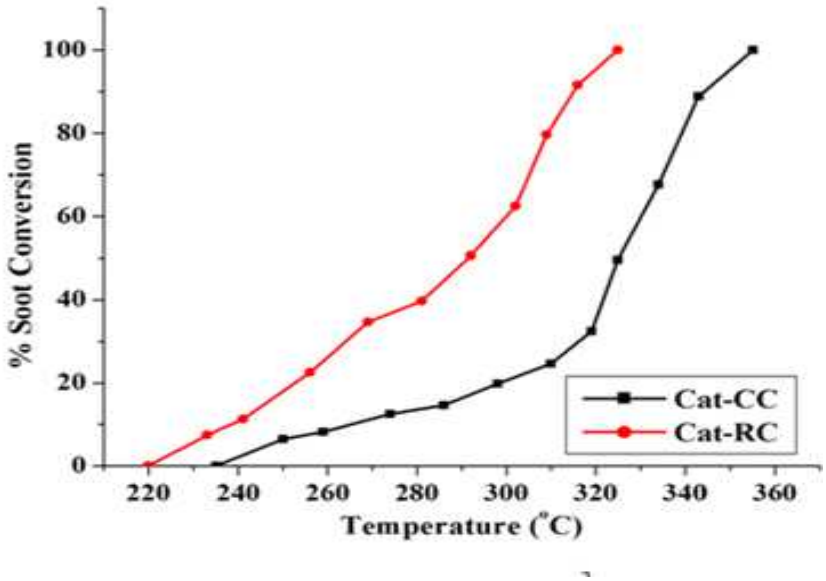

Figure 7.9 Conversion of soot with Air and RC- $La_{0.9}Sr_{0.1}Co_{0.5}Fe_{0.5}O_{3-\delta}$ Perovskite Catalysts

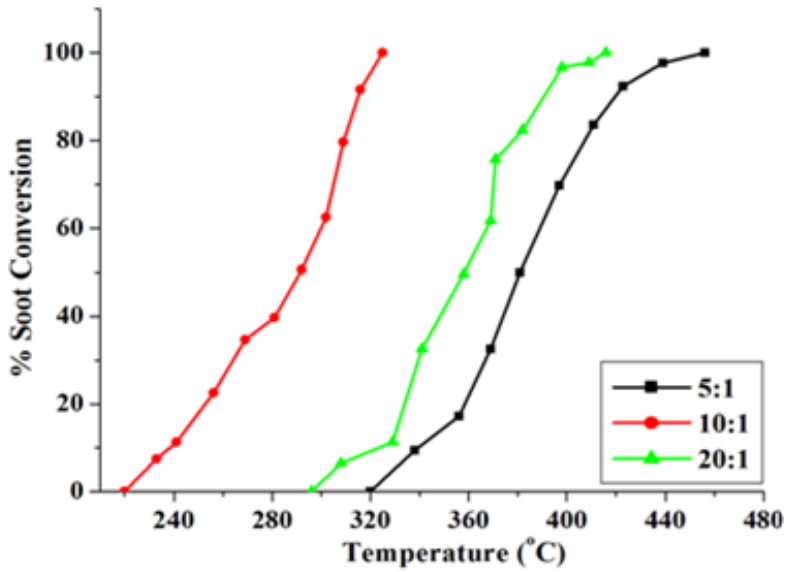

Figure 7.10 Conversion of soot with different Cat-Soot ratio over RC-$La_{0.9}Sr_{0.1}Co_{0.5}Fe_{0.5}O_{3-\delta}$

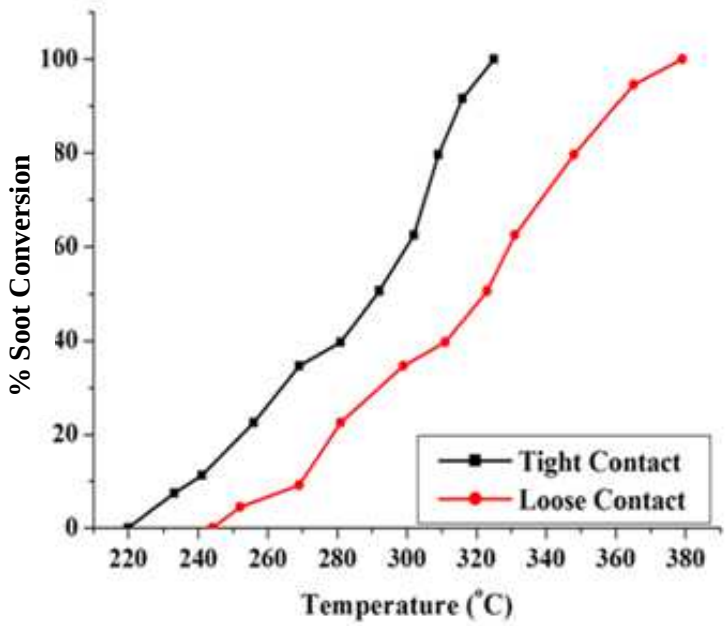

Figure 7.11 Conversion of soot with different Cat-Soot Contact Conditions over RC-$La_{0.9}Sr_{0.1}Co_{0.5}Fe_{0.5}O_{3-\delta}$

Both the catalysts were selective for CO_2 as no CO was detected in the flue stream and showed total combustion of soot within the diesel exhaust range of 150-450^{o}C (figure 7.9). It is very clear from figure 7.9 and table 7.4, that the double substituted catalyst

formulation $La_{0.9}Sr_{0.1}Co_{0.5}Fe_{0.5}O_{3-\delta}$, obtained by RC showed the higher activities than the catalyst produced by calcinations in stagnant air. RC-catalyst exhibited the best performance resulting total soot combustion at the lowest temperature of 325^{o}C. The best performance of RC-catalyst was associated with its unusual textural and morphological characteristics as well as partially reduced perovskite structure. RC caused partial reduction of perovskite leading to lattice vacancies and lattice defects consequently ensuing high density of active sites in the catalyst. The perovskite structure remains unaltered for all the substituted catalysts prepared in the present study. To verify the reproducibility of the experimental data each experiment was performed at least twice repeatedly for the soot oxidation and the data were found to be reproducible within ± 1% of deviation. The experiments were also performed over $La_{0.9}Sr_{0.1}Co_{0.5}Fe_{0.5}O_{3-\delta}$-RC to optimize the catalyst-soot ratio (Figure 7.10) and table 7.5). The activity order of the catalyst in decreasing sequence was as follows: 10:1>5:1>20:1. A loose contact study was also carried out to simulate the actual circumstances of diesel particulate filter [Guillen hurtado et al. 2014]. Figure 7.11 shows a comparison of conversion of soot particles over $La_{0.9}Sr_{0.1}Co_{0.5}Fe_{0.5}O_{3-\delta}$-RC under tight and loose contacts conditions of the catalyst-soot. It can be visualized from figure 7.11 that loose contact exhibited lower activity than tight contact. The observation is obvious as the catalysis is a surface phenomenon, higher the surface contacts (tight contact) higher the activity. From the table 7.6 it is clear that Cat-R resulted complete soot oxidation at T_f = 379^{o}C under loose contact which is 54^{o}C higher than tight contact. The catalytic activity for soot oxidation under loose contact conditions is found to be very much appreciating within the diesel exhaust conditions i.e. < 450^{o}C. Thus, it should be effective to oxidize the soot on coating over DPF in real diesel engine exhaust.

Table 7.4 Characteristic light off temperature for soot oxidation over perovskite catalysts

Catalyst	**T_i(^{o}C)**	**T_{50}(^{o}C)**	**T_f(^{o}C)**
Cat-CC	238	330	355
Cat-RC	220	308	325

Table 7.5 Characteristic light off temperature for soot oxidation over Cat-RC with different cat soot ratio

C/S ratio	**T_i(^{o}C)**	**T_{50}(^{o}C)**	**T_f(^{o}C)**
5:1	320	381	456
10:1	220	308	325
20:1	296	359	416

Table 7.6 Light off temperatures on $La_{0.9}Sr_{0.1}Co_{0.5}Fe_{0.5}O_{3-\delta}$-RC under different catalyst-soot contacts

Contact Type	**T_i(^{o}C)**	**T_{50}(^{o}C)**	**T_f(^{o}C)**
Tight contact	220	308	325
Loose contact	244	329	379

7.3.8 Thermal stability of the Catalyst

Further experiments were conducted to examine the thermal stability of typical $La_{0.9}Sr_{0.1}Co_{0.5}Fe_{0.5}O_3$-RC by consecutive soot combustion for five cycles, and the results are shown in Table 6. It is evident from the table that the catalyst maintained its high catalytic activity for repeated five cycles under the condition of tight contact between catalysts and soot particles. The variation in the light off temperature of soot oxidation values of T_i, T_{50} and T_f are within the experimental error (table 7.7). The result indicates that the catalyst has good thermal stability for soot oxidation.

Table 7.7 Stability test of catalyst Cat-RC for soot combustion under tight contact

Test Cycle	T_i(^{o}C)	T_{50}(^{o}C)	T_f(^{o}C)
1st	220	308	325
2nd	221	307	324
3rd	219	307	326
4th	220	309	325
5th	221	308	324

7.4 Conclusions

A novel route of single step reactive calcination of catalyst precursors far below their decomposition temperatures for the synthesis of highly active catalysts for soot oxidation is investigated. The catalyst produced following the novel route was more active than the ones prepared by the traditional method. The novelty of the catalyst produced by RC is associated with the presence of structural deffects and unusual morphology. The $La_{0.9}Sr_{0.1}Co_{0.5}Fe_{0.5}O_{3-\delta}$ calcined in reactive atmosphere reveals the low temperature (T_f= 325^{o}C) than the Cat-CC calcined in air for total soot oxidation. The high catalytic activity of Fe-substituted Cat-RC perovskite catalysts can be explicated from following aspects: firstly, the catalysts and the soot particulates fall in the nano-metric range, which ensure the high contact efficiency between them; secondly, the textural defects and oxygen vacancies created by partial reduction of the perovskite structure which is confirmed by the XPS analysis, increases the oxidation ability of the catalysts.